Hindawi
Mathematical Problems in Engineering
Volume 2022, Article ID 7980267, 10 pages
https://doi.org/10.1155/2022/7980267

Research Article

Unsteady MHD Williamson Fluid Flow with the Effect of Bioconvection over Permeable Stretching Sheet

Muhammad Imran Asjad,[1] **Muhammad Zahid**,[1] **Bagh Ali**,[2] **and Fahd Jarad**[3,4,5]

[1]*Department of Mathematics, University of Management and Technology, Lahore 54770, Pakistan*
[2]*Department of Applied Mathematics, Northwestern Polytechnical University, Xi'an 710072, China*
[3]*Department of Mathematics, Cankaya University, 06790 Etimesgut, Ankara, Turkey*
[4]*Department of Mathematics, King Abdulaziz University, Saudi Arabia*
[5]*Department of Medical Research, China Medical University Hospital, China Medical University, Taichung, Taiwan*

Correspondence should be addressed to Fahd Jarad; fahd@cankaya.edu.tr

Received 20 October 2021; Revised 15 August 2022; Accepted 15 September 2022; Published 3 October 2022

Academic Editor: Muhammad Irfan

The unsteady flow of Williamson fluid with the effect of bioconvection in the heat and mass transfer occurring over a stretching sheet is investigated. A uniform magnetic field, thermal radiation, thermal dissipation, and chemical reactions are taken into account as additional effects. The physical problem is formulated in the form of a system of partial differential equations and solved numerically. For this purpose, similarity functions are involved to transmute these equations into corresponding ordinary differential equations. After that, the Runge-Kutta method with shooting technique is employed to evaluate the desired findings with the utilization of a MATLAB script. As a result, the effects of various physical parameters on the velocity, temperature, and nanoparticle concentration profiles as well as on the skin friction coefficient and rate of heat transfer are discussed with the aid of graphs and tables. The parameters of Brownian motion and thermophoresis are responsible for the rise in temperature and bioconvection Rayleigh number diminishes the velocity field. This study on nanofluid bioconvection has been directly applied in the pharmaceutical industry, microfluidic technology, microbial improved oil recovery, modelling oil and gas-bearing sedimentary basins, and many other fields. Further, to check the accuracy and validation of the present results, satisfactory concurrence is observed with the existing literature.

1. Introduction

The complicated and fast processes in heavy machinery and small gadgets have created a serious problem of thermal imbalance. Various extraneous techniques, such as fins and fans, have been employed, but their utility is limited due to their large size. In 1995, Choi and Eastman [1] introduced nano-sized particles mixed in the fluid called nanofluid, which has more capacity for heat transfer as compared to fluid without nano-sized particles. Nanofluid has attained impressive consideration because of its huge applications in the fields of technology and engineering. Das et al. [2] discuss recent and future applications of fluids containing nano-sized particles. Turkyilmazoglu and Pop [3] examined the thermal and mass transportation influences on some natural convection streams of unsteady MHD nanofluids with the effect of radiation taken into account. Khan et al. [4] used the shooting method analyzed flow features of Williamson nanofluid influenced by variable viscosity depending on temperature and Lorentz force past an inclined nonlinear extending surface and also via graphically discussed the variable viscosity, mixed convection, Brownian motion, Lewis number, Prandtl number, Sherwood number, and Nusselt number. Sui et al. [5] introduced the Cattaneo-Christov model with double diffusion to analyze the significance of slip velocity, Brownian motion, thermophoresis, mass, thermal transportation, and variable viscosity in the stream of Maxwell upper convected

nanofluid over an extending surface using HAM. Izadi et al. [6] investigated the numerically thermogravitational convection of micropolar MHD nanofluid having thermal radiation and a magnetic field past a porous chamber in the presence of an elliptical heated cylinder.

Aman et al. [7] investigated the effects of a magnetic field, heat transfer, and slip conditions on the flow of MHD incompressible and viscous fluid through a converging/diverging medium. Hsiao [8] described the flow property of a 2-D electrically conducting micropolar nanofluid past an extending permeable surface with the magnetic field, mass, thermal transportation, viscous dissipation, and MHD effects taken into account. The significance of chemical reaction, heat source, viscous dissipation, thermal radiation, suction, and magnetic field on mixed convection flow of hydromagnetic Casson nanofluid through a nonlinear extending porous medium has been discussed by Ibrahim et al. [9]. Fatunmbi et al. [10] examined the reactive stream of micropolar MHD fluid through a permeable extending sheet having effects on concentration and thermal slip boundary conditions. Hayat et al. [11] studied the flow features of third-grade electrically conducting MHD nanofluid over a stretching sheet in the presence of activation energy, chemical reaction, convective boundary, and magnetic field effects. Mousavi et al. [12] described a novel combination of theoretical and experimental models that provides dual solutions for Casson hybrid nanofluid flow caused by a stretching/shrinking sheet. Jabbarpour et al. [13] investigated the issue of stable general three-dimensional magnetohydrodynamics stagnation-point boundary layer flow via an impermeable wavy circular cylinder using an aluminum-copper/water hybrid nanofluid as the working fluid and boundary conditions of velocity slip and temperature jump. Izady et al. [14] scrutinized the development of the Falkner-Skan problem is the flow of an aqueous Fe2O3-CuO/water hybrid nanofluid across a permeable stretching/shrinking wedge.

Hayat et al. [15] described the impact of second-grade magnetized nanofluid and the characteristics of mass and heat transfer due to stretching sheets using convective boundary conditions. Goud et al. [16] examined stagnation-point magnetohydrodynamics flow past an extending surface because of a slip boundary and thermal radiation. Srinivasulu and Goud [17] calculated mass and thermal transport in a Williamson nanofluid stream past a stretching surface with convective boundary and magnetic field effects. Khan and Nadeem [18] scrutinized the rotating stream of Maxwell nanofluid with activation energy and double diffusion through stretching sheets influenced by centrifugal, thermophoresis, and Coriolis forces.

Bioconvection describes the phenomenon in which living microorganisms denser than water swim upward in suspensions. These microorganisms pileup in the layer of the upper surface and, because of this pileup, the lower surface becomes less dense than the upper surface and the distribution of density becomes unstable due to the microorganisms falling into it, and phenomena of bioconvection occur. Bioconvection has applications in biological systems and biotechnology, such as purifying cultures, enzyme biosensors, and separating dead and living cells [19]. Raees et al. [20] examined the unsteady stream of bioconvection-mixed nanofluid containing gyrostatic motile microorganisms through a horizontal channel. Siddiqa et al. [21] numerically studied the bioconvection flow of nanofluid having mass and thermal transportation along with gyrotactic microorganisms through a curved vertical cone.

Abbasi et al. [22] introduced the bioconvection stream of viscoelastic nanofluid because of gyrotactic microorganisms past a rotating extending disc having zero-mass flux and convective boundary condition and also described the relatable parameters' influences on velocity, temperature, local density, Sherwood number, and Nusselt number in detail. Chu et al. [23] developed the Buongiorno model to analyze the stream of 2-D MHD bioconvection third-grade fluid along an extending sheet with the significance of motile microorganisms, activation energy, thermophoresis diffusion, Brownian motion, chemical reaction, and magnetic field taken into account. Henda et al. [24] examined the magnetized bioconvection flow of third-grade fluid past an extending cylinder with thermal radiation, activation energy, and a heat source. The effects of thermophoresis and Brownian motion are also discussed. Khan et al. [25] applied the numerical method bpv4c to a scrutinized stream of viscous bioconvection nanofluid through multiple geometries with heat flux, cross-diffusion, and Cattaneo-Christov, as well as Brownian motion, thermophoresis diffusion, and concentration gradients.

Because of its importance in engineering and industrial processes, non-Newtonian fluids compel researchers to investigate the phenomena of mass and heat transport. Shampoos, jelly, sugar, honey, human blood, pulps, and other non-Newtonian fluids are examples. Williamson fluid is also a category of the fluid model that is pseudo-plastic. Pseudo-plastic fluids have applications in the engineering and industrial fields, such as food processing, blood cells, photographic films, and inkjet printing. Li et al. [26] examined the combined effects of MHD and magnetic field on the stream of Williamson nanofluid through exponentially extending permeable sheets with heat generation/absorption. Hamid [27] investigated the influence of Brownian motion and thermophoresis on Williamson MHD nanofluid flow through a wedge using the zero-mass flux and convective boundary. Rasool et al. [28] scrutinized the Buongiorno model to discuss the flow behavior of reactive Williamson MHD nanofluid because of Brownian motion and thermophoresis over a nonlinear permeable sheet. Kumar et al. [29] introduced viscous dissipation, thermal radiation nonlinearly, joule heating, and magnetic field to analyze the stream of Williamson nanofluid past an extending sheet influenced by chemical reactions. Shateyi and Muzara [30] analyzed a thorough and detailed study of the incompressible conductive Williamson nanofluid on the extending permeable sheet. Ali et al. [31] investigated the effects of thermal diffusion, thermal radiation, and MHD on the time-dependent flow of a Maxwell nanofluid past an extending geometry using FEM.

Sindhu and Atangana [32] discussed the framework to model the efficiency and functionality lifespan of electronic

equipment with reliability analysis. Rehman et al. [33] discussed time-censored data and statistical inference for the Burr type X distribution in an accelerated life testing design using a geometric process. Shafiq et al. [34] simulated an effective statistical distribution to examine COVID-19 death rates in Canada and the Netherlands. Sindhu et al. [35] studied modelling of COVID-19 data using an exponentiated transformation of the Gumbel Type-II distribution. Shafiq et al. [36] scrutinized artificial neural network optimization of Darcy-Forchheimer squeezing flow in a nonlinear stratified fluid under convective conditions. Shafiq et al. [37] studied numerical and artificial neural network models to estimate unsteady hydromagnetic Williamson fluid flow on a radiative surface.

In most of the previous studies, the bioconvection of an unsteady Williamson nanofluid was rarely studied. The key aim of the current work is to examine the behavior of bioconvection impacts on Williamson MHD nanofluid transportation over an extending permeable sheet with the insertion of gyrotactic auto-motile organisms to avoid possible settling of nano entities. This investigation is relevant to high-temperature nanomaterial processing technology. Actually, common base fluids bear low thermal conductivity and thus, lose their practical importance. Nanoparticles may improve thermal transport in emerging sophisticated heat exchanger electronics. Bioconvection is presumed to inhibit the sedimentation of nano entities. The connotation of such meaningful attributes can be a useful extension and the results can be utilized for the desired effective thermal transportation in the heat exchanger of various technological processes.

2. Problem Formulation

Here we consider the flow of non-Newtonian Williamson nanofluids on the wall of sheet stretches with velocity $\widetilde{U_w} = cx/(1-at)$ along the x-axis and y-axis taken to be normal,

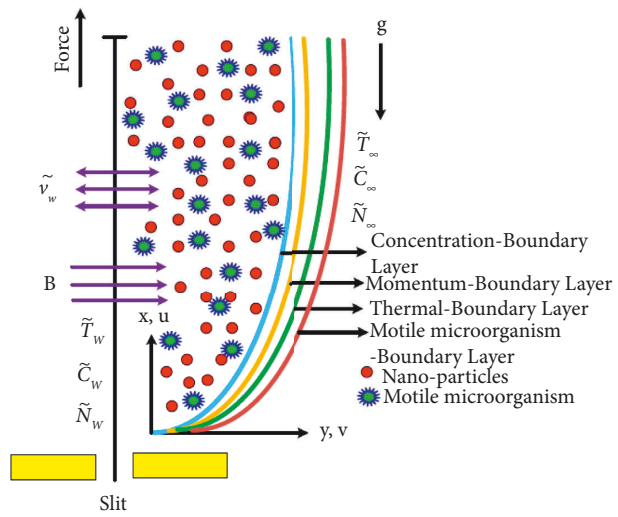

Figure 1: Geometry of the problem [38].

where $c>0$ is the rate of stretching along the x-axis. $\vec{B} = (0, B_0, 0)$ denotes the magnetic field applied to the flow region and acts in the y-direction. A mild diffusion of microorganisms and nanoparticles is set in the non-Newtonian base fluid. Thermal radiation is considered and bioconvection takes place because of microorganism's movement as shown in Figure 1 [38]. The fluid velocity component for two dimensional flow is $\tilde{u}, \tilde{v}$ the temperature is $\tilde{T}$, nanoparticle concentration is $\tilde{C}$, and microorganisms density is $\tilde{N}$. The appropriate governing equations are given [30, 31, 39].

Continuity equation:

$$\frac{\partial \tilde{u}}{\partial x} + \frac{\partial \tilde{v}}{\partial y} = 0. \tag{1}$$

Momentum equation:

$$\frac{\partial \tilde{u}}{\partial t} + \tilde{u}\frac{\partial \tilde{u}}{\partial x} + \tilde{v}\frac{\partial \tilde{u}}{\partial y} = \vartheta\frac{\partial^2 \tilde{u}}{\partial y^2} + 2\vartheta\Gamma\frac{\partial \tilde{u}}{\partial y}\frac{\partial^2 \tilde{u}}{\partial y^2} - \frac{\sigma}{\rho}\left(B_0^2\tilde{u}\right) + \frac{1}{\rho}\left[g\beta\rho\left(1-\widetilde{C_\infty}\right)\left(\tilde{T}-\widetilde{T_\infty}\right) - g\left(\rho_p-\rho_f\right)\left(\tilde{C}-\widetilde{C_\infty}\right) - g\gamma\left(\tilde{N}-\widetilde{N_\infty}\right)\right]. \tag{2}$$

Heat equation

$$\frac{\partial \tilde{T}}{\partial t} + \tilde{u}\frac{\partial \tilde{T}}{\partial x} + \tilde{v}\frac{\partial \tilde{T}}{\partial y} = \frac{K}{\rho C_p}\frac{\partial^2 \tilde{T}}{\partial y^2} + \frac{\mu}{\rho C_p}\left(\frac{\partial \tilde{u}}{\partial y}\right)^2 + \frac{\mu\Gamma}{\rho C_p}\left(\frac{\partial \tilde{u}}{\partial y}\right)^3 + \frac{\sigma}{\rho C_p}\left(\beta_0\tilde{u}\right)^2 - \frac{1}{\rho C_p}\frac{\partial q_r}{\partial y} + \tau\left(D_B\frac{\partial \tilde{T}}{\partial y}\frac{\partial \tilde{C}}{\partial y} + \frac{D_T}{\widetilde{T_\infty}}\left(\frac{\partial \tilde{T}}{\partial y}\right)^2\right). \tag{3}$$

Concentration equation

$$\frac{\partial \tilde{C}}{\partial t} + \tilde{u}\frac{\partial \tilde{C}}{\partial x} + \tilde{v}\frac{\partial \tilde{C}}{\partial y} = D\frac{\partial^2 \tilde{C}}{\partial y^2} - K_r\left(\tilde{C}-\tilde{C}_\infty\right) + \frac{D_T}{\widetilde{T_\infty}}\frac{\partial^2 \tilde{T}}{\partial y^2}. \tag{4}$$

Bioconvection equation

$$\frac{\partial \tilde{N}}{\partial t} + \tilde{u}\frac{\partial \tilde{N}}{\partial x} + \tilde{v}\frac{\partial \tilde{N}}{\partial y} + dW_c\left(\frac{\tilde{N}}{\nabla\tilde{C}}\frac{\partial \tilde{C}}{\partial y}\right) = D_n\frac{\partial^2 \tilde{N}}{\partial y^2}, \tag{5}$$

with the boundary conditions

$$\begin{aligned}
&\widetilde{u}(x,0) = \widetilde{U}_w,\\
&\widetilde{v}(x,0) = \widetilde{V}_w,\\
&\widetilde{T}(x,0) = \widetilde{T}_w,\\
&\widetilde{C}(x,0) = \widetilde{C}_w,\\
&\widetilde{N}(x,0) = \widetilde{N}_w,\\
&\widetilde{u} \longrightarrow 0,\ \widetilde{T} \longrightarrow \widetilde{T}_\infty,\ \widetilde{C} \longrightarrow \widetilde{C}_\infty,\\
&\widetilde{N} \longrightarrow \widetilde{N}_\infty,\ \text{as} y \longrightarrow \infty,\\
&\widetilde{T}_w(x,t) = \widetilde{T}_\infty + \frac{cx}{2\vartheta(1-at)^2}\widetilde{T}_0,\\
&\widetilde{C}_w(x,t) = \widetilde{C}_\infty + \frac{cx}{2\vartheta(1-at)^2}\widetilde{C}_0,\\
&\widetilde{N}_w(x,t) = \widetilde{N}_\infty + \frac{cx}{2\vartheta(1-at)^2}\widetilde{N}_0,
\end{aligned} \tag{6}$$

where $\widetilde{c} \geqslant 0$. $\widetilde{T}_0\,(0 \leqslant \widetilde{T}_0 \leqslant \widetilde{T}_w)$, $\widetilde{C}_0\,(0 \leqslant \widetilde{C}_0 \leqslant \widetilde{C}_w)$, and $\widetilde{N}_0\,(0 \leqslant \widetilde{N}_0 \leqslant \widetilde{N}_w)$ are the reference temperature, concentration, and bioconvection, respectively.

Roseland approximations [30],

$$q_r = \frac{4o^*}{3k_1}\frac{\partial \widetilde{T}^4}{\partial y}, \tag{7}$$

where σ^* is the Stefan-Boltzmann constant and k_1 is the mean absorption coefficient. Applying Taylor's series, we have $\widetilde{T}^4 \simeq 4\widetilde{T}_\infty^3\widetilde{T} - 3\widetilde{T}_\infty^4$, where $\widetilde{T}_\infty$, is the ambient temperature and the energy (3) becomes

$$\begin{aligned}
\frac{\partial \widetilde{T}}{\partial t} + \widetilde{u}\frac{\partial \widetilde{T}}{\partial x} + \widetilde{v}\frac{\partial \widetilde{T}}{\partial y} &= \frac{1}{\rho C_p}\left(\frac{16\sigma^*\widetilde{T}_\infty^3}{3k_1} + K\right)\frac{\partial^2 \widetilde{T}}{\partial y^2}\\
&+ \frac{\mu}{\rho C_p}\left(\frac{\partial \widetilde{u}}{\partial y}\right)^2 + \frac{\mu\Gamma}{\rho C_p}\left(\frac{\partial \widetilde{u}}{\partial y}\right)^3 + \frac{\sigma}{\rho C_p}(\beta_0\widetilde{u})^2.
\end{aligned} \tag{8}$$

Consider the following similarity transformation [30, 39]:

$$\begin{aligned}
\eta &= \sqrt{\frac{\widetilde{U}_w}{x\vartheta}}y,\\
\psi &= \sqrt{\vartheta x\widetilde{U}_w}f(\eta),\\
\theta(\eta) &= \frac{\widetilde{T} - \widetilde{T}_\infty}{\widetilde{T}_w - \widetilde{T}_\infty},\\
\phi(\eta) &= \frac{\widetilde{C} - \widetilde{C}_\infty}{\widetilde{C}_w - \widetilde{C}_\infty},\\
\chi(\eta) &= \frac{\widetilde{N} - \widetilde{N}_\infty}{\widetilde{N}_w - \widetilde{N}_\infty}.
\end{aligned} \tag{9}$$

With the velocity components given by $\widetilde{u} = \partial\psi/\partial y$ and $\widetilde{v} = -\partial\psi/\partial x$ where ψ is the stream function.

Dimensionless momentum equation:

$$\begin{aligned}
&(1 + 2We f'')f''' + ff'' - (f')^2 - S\left(f' + \frac{\eta}{2}f''\right)\\
&- M^2(f') + \lambda(\theta - Nr\phi - Rb\chi) = 0.
\end{aligned} \tag{10}$$

Dimensionless energy equation:

$$\begin{aligned}
&\frac{1}{\Pr}\left(1 + \frac{4R}{3}\right)\theta'' + f\theta' - \frac{S\eta}{2}\theta' - (2S + f')\theta\\
&+ Ec\left((f'')^2 + We(f'')^3\right) + M^2 Ec(f')^2\\
&+ Nb\theta'\phi' + Nt(\theta')^2 = 0.
\end{aligned} \tag{11}$$

Dimensionless concentration equation:

$$\frac{1}{Sc}\phi'' + \left(f - \frac{S\eta}{2}\right)\phi' + (2S - f' - \gamma)\phi = 0. \tag{12}$$

Dimensionless bioconvection equation

$$\chi'' + Lb\Pr f\chi' - Lb\Pr f'\chi - Pe\sigma\phi'' + \chi\phi'' + \chi'\phi' = 0. \tag{13}$$

The corresponding boundary conditions becomes

$$\begin{aligned}
&f(0) = f_w,\\
&f'(0) = 1,\\
&\phi(0) = 1,\\
&\chi(0) = 1,\\
&f'(\infty) \longrightarrow 0,\ f''(\infty) \longrightarrow 0,\ \theta(\infty) \longrightarrow 0,\\
&\phi(\infty) \longrightarrow 0,\ \chi(\infty) \longrightarrow 0.
\end{aligned} \tag{14}$$

The flow characteristics which are of engineering significance are the skin friction coefficient, the local Nusselt number, and the Sherwood number, which are defined, respectively:

$$\begin{aligned}
C_f &= \frac{\tau_w}{\rho U_w^2},\\
Nu_x &= \frac{xq_w}{K\left(\widetilde{T_w} - \widetilde{T_\infty}\right)},\\
Sh_x &= \frac{xj_w}{k_\infty\left(\widetilde{C_w} - \widetilde{C_\infty}\right)}.
\end{aligned} \tag{15}$$

Upon applying the necessary expressions for τ_w, q_w, and j_w, we get the following:

Table 1: Comparison of $C_f \mathrm{Re}_x^{(1/2)}$ (skin friction coefficient) - $f''(0)$ with variation of magnetic parameter M when f_w, λ, Nr, Rb, We, $S = 0$.

M	Ali et al. [31] using FEM	Our results using R-K
0.0	1.0000080	1.0000084
0.2	1.0954458	1.0954460
0.5	1.2247446	1.2247449
1.0	1.4142132	1.4142136
1.2	1.4832393	1.4832397
1.5	1.5811384	1.5811388
2.0	1.7320504	1.7320508

Table 2: Comparison of $Nu_x \mathrm{Re}_x^{-(1/2)}$ (Nusselt number) $-\theta'(0)$ values for Prandtl number Pr and other parameter f_w, λ, Nr, Rb,S, Ec, Nb, Nt,R, We,M, $\delta_2 = 0$.

Pr	Mabood and Shateyi, [40] using FDM	Ali et al. [31] using FEM	Our results using R-K
0.72	0.8088	0.8086339299	0.808834203980
1.00	1.0000	1.0000080213	1.000008368634
3.00	1.9237	1.9236777221	1.923678653470
10.00	3.7207	3.7206681683	3.720671163991
100.00		12.294051659	12.294081083857

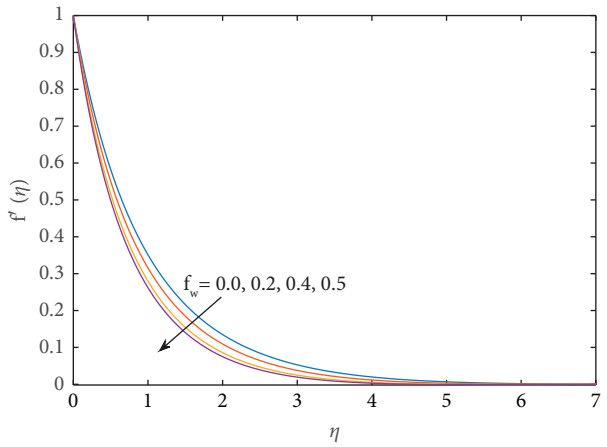

Figure 2: Influence of f_w on f' where $M = 0.5, S = 0.5, R\ d = 1.0, \mathrm{Pr} = 1.1, Nb = 0.1, Nt = 0.1, Le = 1, Nr = 0.3, Rb = 0.1, We = 0.1, pe = 1.0$.

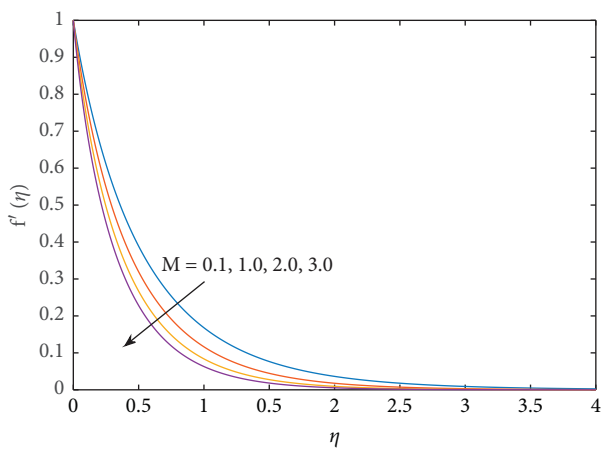

Figure 3: Influence of M on f' where $f_w = 0.5, S = 0.5, R\ d = 1.0, \mathrm{Pr} = 1.1, Nb = 0.1, Nt = 0.1, Le = 1, Nr = 0.3, Rb = 0.1, We = 0.1, pe = 1.0$.

$$C_f = \mathrm{Re}_x^{-1/2}\left[f''(0) + We f'^2(0)\right],$$
$$Nu_x = -\mathrm{Re}_x^{1/2}\left(1 + \frac{4R}{3}\right)\theta'(0), \tag{16}$$
$$Sh_x = -\mathrm{Re}_x^{1/2}\phi'(0).$$

The basic discretization methods are FDM (finite difference method), FVM (finite difference method), and FEM (finite element method). However, the computational cost and time of these methods are much higher for the determination of the unknowns, but the Runge-Kutta method is cost-effective and efficient. The Runge-Kutta method is widely used to solve ordinary differential equations. Runge-Kutta (R-K) methods with shooting techniques have been widely utilized for the solution of flow problems. This method with the shooting technique is a powerful scheme for solving ODEs. In short, the Runge-Kutta method solves the boundary value problems adequately, rapidly, and precisely. Thus, the relative simplicity and low computational cost have made this numeric scheme widely applied in the nonlinear analysis of applied science.

3. Results and Discussion

The physical meanings of the final nondimensional formulation of time-dependent MHD flow of Williamson nanofluid due to the stretch of a horizontal sheet in the presence of bioconvection and chemical reaction along the boundary constraints are solved numerically as described in the above segment. It is because inherent nonlinearity and coupling make the boundary value problem difficult to yield an exact solution. The pertinent parameters are varied in an appropriate range to reveal their influence on dependent variables for the concentration of nanoparticles, fluid temperature, microorganism distribution, and fluid velocity.

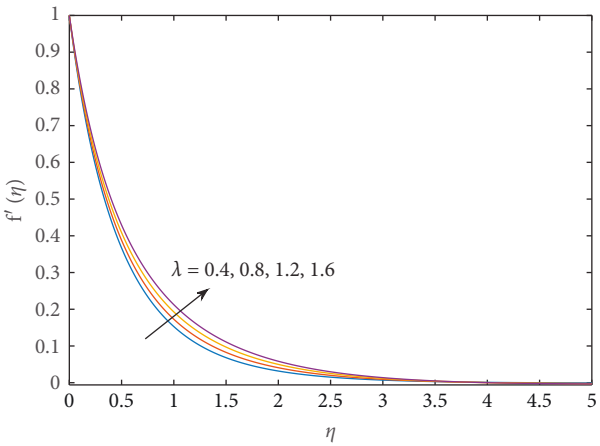

Figure 4: Influence of λ on $f\prime$ where $M = 0.5$, $f_w = 0.5$, $S = 0.5, R\,d = 1.0, \mathrm{Pr} = 1.1, Nb = 0.1,\ Nt = 0.1, Le = 1, Nr = 0.3, Rb = 0.1, We = 0.1, pe = 1.0$.

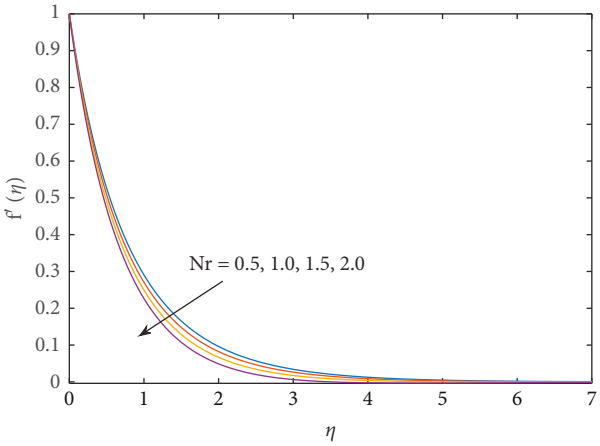

Figure 5: Influence of Nr on $f\prime$ where $M = 0.5$, $f_w = 0.5, S = 0.5$, $R\,d = 1.0, \mathrm{Pr} = 1.1, Nb = 0.1, Nt = 0.1, Le = 1, Rb = 0.1, We = 0.1$, $pe = 1.0$.

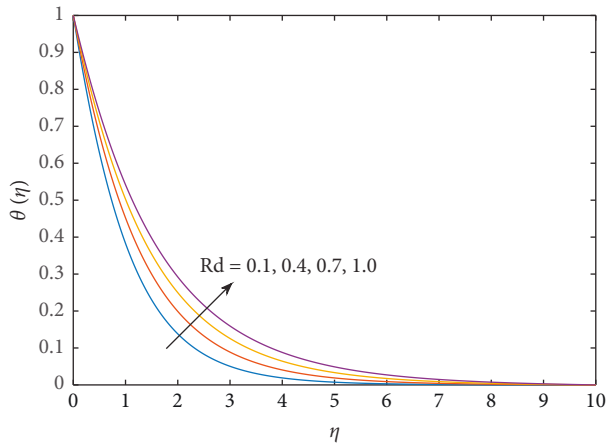

Figure 6: Influence of Rd on θ where $M = 0.5$, $f_w = 0.5, S = 0.5$, $\mathrm{Pr} = 1.1$, $Nb = 0.1$, $Nt = 0.1, Le = 1, Rb = 0.1, We = 0.1$, $pe = 1.0$.

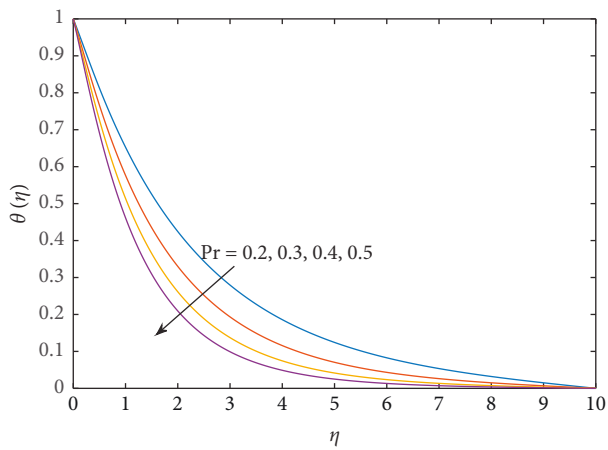

Figure 7: Influence of Pr on θ where $M = 0.5$, $f_w = 0.5, S = 0.5$, $Nb = 0.1, Nt = 0.1, Le = 1, Rb = 0.1, We = 0.1$, $pe = 1.0$.

To ensure the validation of the numeric procedure, current results are compared with those in the existing literature as limiting cases. The comparative output for skin friction factor $-f''(0)$ is shown in Table 1. For the present case and those of Ali et al. [31]. Table 2 contains present results for Nusselt number $-\theta'(0)$ when compared with Fazle and Shateyi [40] and Ali et al. [31]. A comparison of the results as depicted in these tables indicates acceptable agreement to validate this numeric procedure.

The velocity plot in Figure 2 depicts the slowing velocity of the fluid as the mass suction attributed with f_w is increased. From Figure 3, the impact of magnetic parameter M on the Williamson nanofluid velocity function is observed. The velocity of the flow seems to be reduced significantly when $M(0.1 \le M \le 0.3)$ is increased. The opposing force, known as the Lorentz force, inhibits the flow.

As shown in Figure 4, increasing the mixed convection parameter λ causes the flow velocity to increase to $f'(\eta)$. The sketches of velocity $f'(\eta)$ as drawn in Figure 5 indicate the slowing pattern of the flow for buoyancy ratio parameter Nr. $(\tilde{T}_w - \tilde{T}_\infty)$ is the reciprocal of the buoyancy ratio parameter. In the boundary layer regime, buoyancy effects are decreased to better display the flow.

The progressive value of the radiation parameter Rd causes a significant increase in the temperature field $\theta(\eta)$ in Figure 6. The greater Rd means a strong radiation mode of heat transfer which helps to raise the temperature.

Because the Prandtl number is inversely proportional to thermal diffusivity, a higher value decreases the degree of temperature $\theta(\eta)$ as shown in Figure 7. Significant rising behavior of $\theta(\eta)$ is observed in Figures 8 and 9 with increased values of Brownian motion parameter Nb and thermophoresis parameter Nt. The fast random motion of nanoparticles characterized by larger Nb is responsible for enhanced heat transfer to raise $\theta(\eta)$. Similarly, the higher Nt means a greater thermophoretic effect, which moves the nanoparticles from the hotter regime to the colder one and increases the thermal distribution.

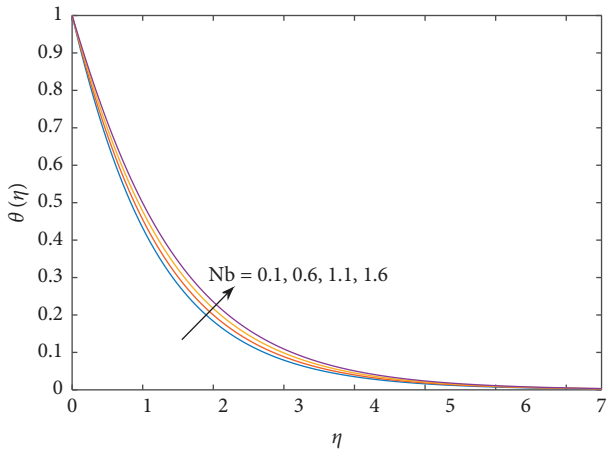

Figure 8: Influence of Nb on θ where $M = 0.5$, $f_w = 0.5$, $S = 0.5$, $Nt = 0.1$, $Le = 1$, Pr $= 1.1$, $Rb = 0.1$, $We = 0.1$, $pe = 1.0$.

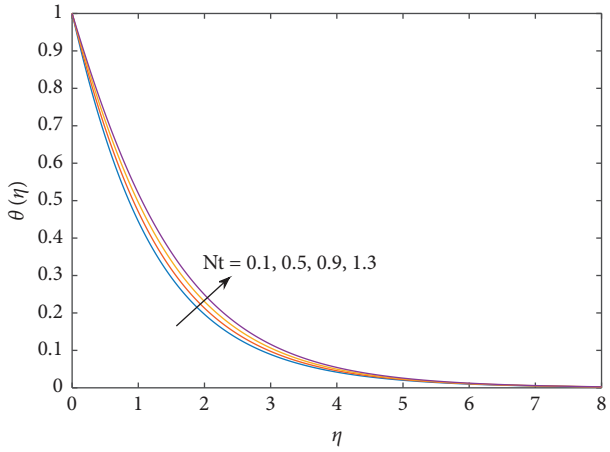

Figure 9: Influence of Nt on θ where $M = 0.5$, $f_w = 0.5$, $S = 0.5$, $Nb = 0.1$, $Le = 1$, Pr $= 1.1$, $Rb = 0.1$, $We = 0.1$, $pe = 1.0$.

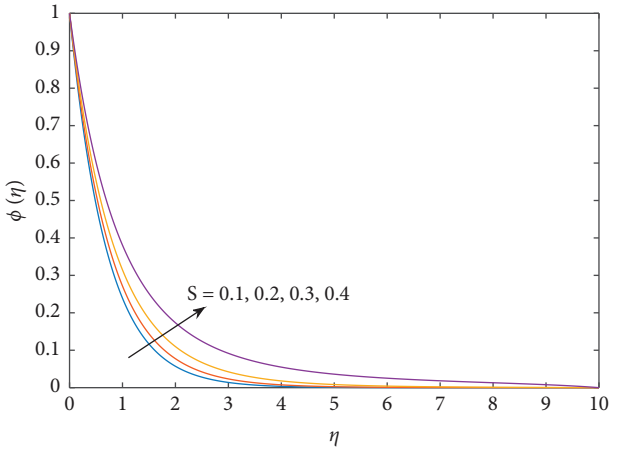

Figure 10: Influence of S on ϕ where $M = 0.5$, $f_w = 0.5$, $Nb = 0.1$, $Nt = 0.1$, $Le = 1$, Pr $= 1.1$, $Rb = 0.1$, $We = 0.1$, $pe = 1.0$.

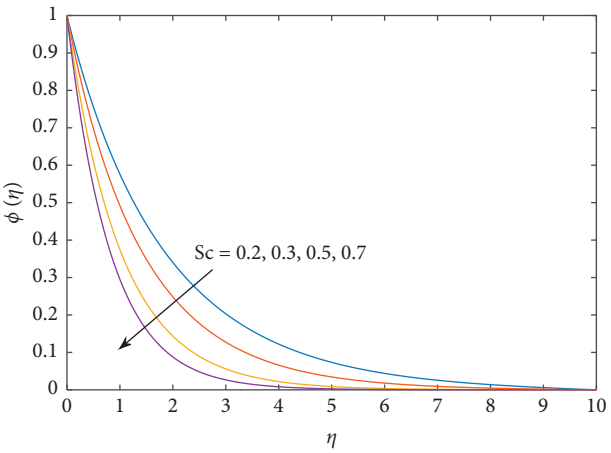

Figure 11: Influence of Sc on ϕ where $M = 0.5$, $f_w = 0.5$, $Nb = 0.1$, $Nt = 0.1$, $Le = 1$, Pr $= 1.1$, $Rb = 0.1$, $We = 0.1$, $pe = 1.0$.

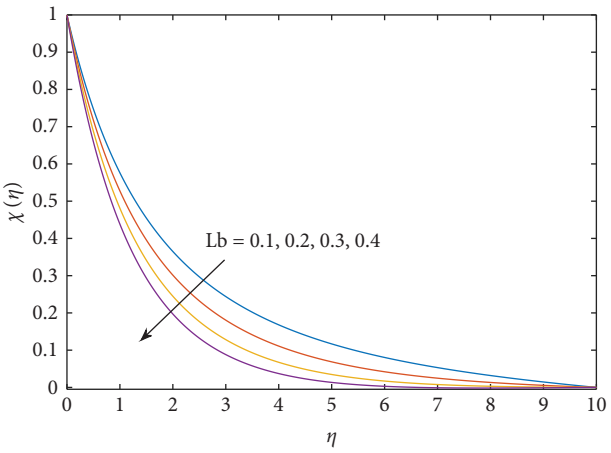

Figure 12: Influence of Lb on χ where $M = 0.5$, $f_w = 0.5$, $Nb = 0.1$, $Nt = 0.1$, $Le = 1$, Pr $= 1.1$, $Rb = 0.1$, $We = 0.1$, $pe = 1.0$.

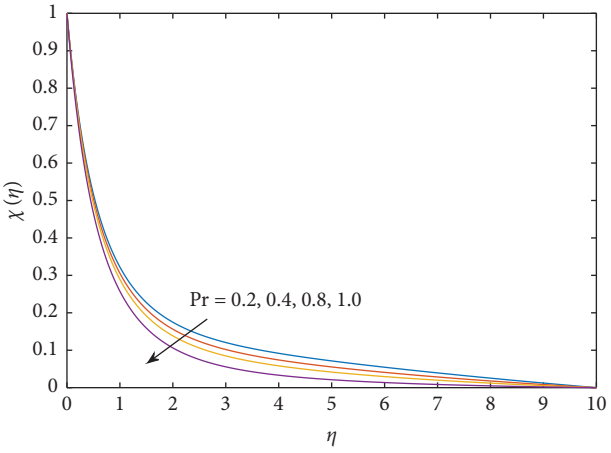

Figure 13: Influence of Pr on χ where $M = 0.5$, $f_w = 0.5$, $Nb = 0.1$, $Nt = 0.1$, $Le = 1$, $Rb = 0.1$, $We = 0.1$, $pe = 1.0$.

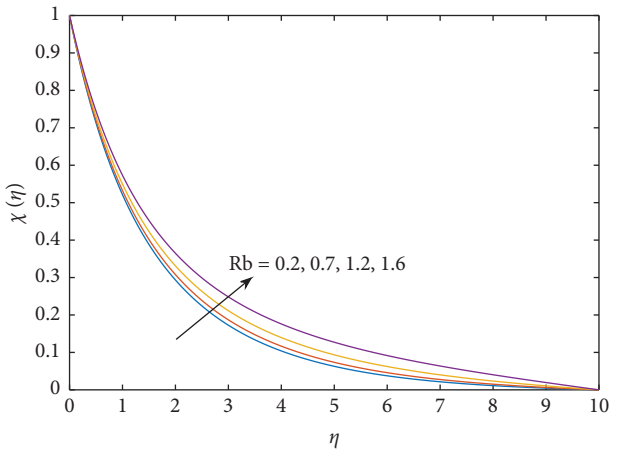

Figure 14: Influence of Rb on χ where $M = 0.5, f_w = 0.5, Nb = 0.1, Nt = 0.1, Le = 1, \Pr = 1.1, We = 0.1, pe = 1.0$.

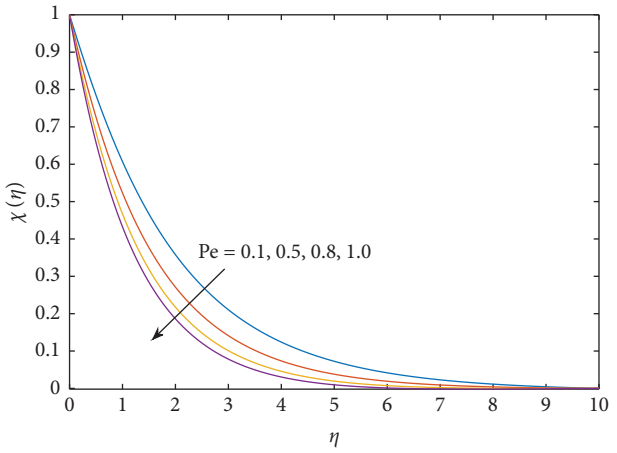

Figure 15: Influence of Pe on χ where $M = 0.5, f_w = 0.5, Nb = 0.1, Nt = 0.1, Le = 1, \Pr = 1.1, Rb = 0.1, We = 0.1$.

In Figure 10 shows the rising behavior of concentration $\phi(\eta)$ indirect relation to the unsteady parameter S. Figure 11 displays the decrement in $\phi(\eta)$ due to the larger value of Schmidt number Sc. The larger Schmidt number means less mass diffusivity to decrease $\phi(\eta)$. From Figure 12, the significant reduction of microorganisms' distribution function $\chi(\eta)$ is attained against improved inputs of bioconvection Lewis number Lb, which is reciprocal to the mass diffusivity of microorganisms. As seems from Figure 13, Prandtl number Pr causes the microorganism's distribution to decline. The bioconvection Rayleigh Rb is responsible for giving a direct increment to $\chi(\eta)$ as demonstrated in Figure 14. As it seems in Figure 15, the larger values of the Peclet number Pe cause the microorganism's distribution to decline.

4. Conclusions

Theoretical and numeric analysis for the magnetohydrodynamics of Williamson nanofluid owing to sudden stretching in a horizontal sheet has been presented in this communication. On the physical field, namely, velocity, temperature, concentration, and microorganism distribution, the effects of the emerging parameters are enumerated. Significant outcomes are summarised as follows:

(i) The velocity, temperature, concentration, and bioconvection parameters are boosted with λ, Rb, Nb, and Nt.

(ii) The velocity, temperature, concentration, and bioconvection parameters reduce with Nr, Lb, and Pe.

(iii) The conclusion of nanoparticles characterized by parameters Nb and Nt shows an increment in the temperature profile. Also, the parameters due to bioconvection have a significant influence on the flow of fluid.

(iv) Further, a study can be carried out with an increment in volume fraction and a non-Newtonian base flow of fluid.

(v) Validation of significant findings and results is debated in Section 3. In the results, satisfactory concurrence is observed when compared with existing literature.

Nomenclature

$S = a/c$:	Unsteadiness parameter
$f_w = v_0/\sqrt{c\vartheta}$:	Suction/injection parameter
$M^2 = \sigma B_0^3(1-at)/\rho a$:	Magnetic parameter
$R = 4\sigma^* \widetilde{T}_\infty^3/kK$:	Thermal radiation parameter
$Sc = \vartheta/D$:	Schmidt number
$Lb = \alpha/D_n$:	Bioconvection lewis number
$Pe = dW_c/D_n$:	Peclet number
$\sigma = \widetilde{N_\infty}/\widetilde{N_w} - \widetilde{N_\infty}$:	Bioconvection parameter
$\Pr = \mu c_p/K$:	Prandtl number
$\gamma = K_r(1-at)/c$:	Chemical reaction parameter
$Ec = \widetilde{U}_w^2/c_p(\widetilde{T}_w - \widetilde{T}_0)$:	Eckert number
$We = \Gamma\widetilde{U}_w\sqrt{c/\vartheta(1-at)}$:	Weissenberg number
$\lambda = (1-\widetilde{C}_\infty)\beta g(\widetilde{T}_w - \widetilde{T}_\infty)2l/U_w^2$:	Mixed convection parameter
$Nr = (\rho_p - \rho_f)(\widetilde{C_w} - \widetilde{C_\infty})/\beta(1 - \widetilde{C_\infty})\rho(\widetilde{T_w} - \widetilde{T_\infty})$	Buoyancy ratio parameter
:	
$Rb = (\rho_m - \rho_f)(\widetilde{N}_w - \widetilde{N}_\infty)/\beta(1-\widetilde{C_\infty})\rho(\widetilde{T}_w - \widetilde{T}_\infty)$	Rayleigh number of bioconvection
:	
$Nt = \tau D_T(\widetilde{T_w} - \widetilde{T_\infty})/\rho\widetilde{T_\infty}$:	Thermophoresis diffusion
$Nb = \tau D_B(\widetilde{C_w} - \widetilde{C_\infty})/\rho$:	Brownian factor
Re:	Reynold's number
$\widetilde{T}$:	Fluid temperature
$\widetilde{T}_w$:	Wall temperature
$\widetilde{T}_\infty$:	

T_∞: Temperature far away from the plate
u: Velocity component along x direction
μ: Dynamic viscosity
ν: Kinematic viscosity.

Data Availability

The data used to support this study are included within this article.

Conflicts of Interest

The authors state that there are no conflicts of interests reported in this work.

Authors' Contributions

All authors contributed equally and significantly to the writing of this paper. All authors read and approved the manuscript.

Acknowledgments

The authors are significantly appreciative and indebted to the University of Management and Technology, Lahore, Pakistan, for enabling and supporting the study effort. The authors extend their appreciation to the Department of Mathematics, Cankaya University, 06790 Etimesgut, Ankara, Turkey.

References

[1] S. U. Choi and J. A. Eastman, "Enhancing thermal conductivity of fluids with nanoparticles," Technical Reports Series, ANL/MSD/CP-84938; CONF-951135-29, Argonne National Lab, IL (United States), 1995.

[2] S. K. Das, S. U. Choi, W. Yu, and T. Pradeep, *Nanofluids: Science and Technology*, John Wiley & Sons, Hoboken, New Jersey, United States, 2007.

[3] M. Turkyilmazoglu and I. Pop, "Heat and mass transfer of unsteady natural convection flow of some nanofluids past a vertical infinite flat plate with radiation effect," *International Journal of Heat and Mass Transfer*, vol. 59, pp. 167–171, 2013.

[4] M. Khan, M. Malik, T. Salahuddin, and A. Hussian, "Heat and mass transfer of Williamson nanofluid flow yield by an inclined lorentz force over a nonlinear stretching sheet," *Results in Physics*, vol. 8, pp. 862–868, 2018.

[5] J. Sui, L. Zheng, and X. Zhang, "Boundary layer heat and mass transfer with cattaneo–christov double-diffusion in upper-convected Maxwell nanofluid past a stretching sheet with slip velocity," *International Journal of Thermal Sciences*, vol. 104, pp. 461–468, 2016.

[6] M. Izadi, M. A. Sheremet, S. Mehryan, I. Pop, H. F. Öztop, and N. Abu-Hamdeh, "MHD thermogravitational convection and thermal radiation of a micropolar nanoliquid in a porous chamber," *International Communications in Heat and Mass Transfer*, vol. 110, Article ID 104409, 2020.

[7] F. Aman, A. Ishak, and I. Pop, "Magnetohydrodynamic stagnation-point flow towards a stretching/shrinking sheet with slip effects," *International Communications in Heat and Mass Transfer*, vol. 47, pp. 68–72, 2013.

[8] K.-L. Hsiao, "Micropolar nanofluid flow with mhd and viscous dissipation effects towards a stretching sheet with multimedia feature," *International Journal of Heat and Mass Transfer*, vol. 112, pp. 983–990, 2017.

[9] S. Ibrahim, G. Lorenzini, P. Vijaya Kumar, and C. Raju, "Influence of chemical reaction and heat source on dissipative mhd mixed convection flow of a casson nanofluid over a nonlinear permeable stretching sheet," *International Journal of Heat and Mass Transfer*, vol. 111, pp. 346–355, 2017.

[10] E. O. Fatunmbi, H. A. Ogunseye, and P. Sibanda, "Magnetohydrodynamic micropolar fluid flow in a porous medium with multiple slip conditions," *International Communications in Heat and Mass Transfer*, vol. 115, Article ID 104577, 2020.

[11] T. Hayat, R. Riaz, A. Aziz, and A. Alsaedi, "Influence of arrhenius activation energy in mhd flow of third grade nanofluid over a nonlinear stretching surface with convective heat and mass conditions," *Physica A: Statistical Mechanics and Its Applications*, vol. 549, Article ID 124006, 2020.

[12] S. M. Mousavi, M. N. Rostami, M. Yousefi, S. Dinarvand, I. Pop, and M. A. Sheremet, "Dual solutions for casson hybrid nanofluid flow due to a stretching/shrinking sheet: a new combination of theoretical and experimental models," *Chinese Journal of Physics*, vol. 71, pp. 574–588, 2021.

[13] B. Jabbaripour, M. N. Rostami, S. Dinarvand, and I. Pop, "Aqueous aluminium–copper hybrid nanofluid flow past a sinusoidal cylinder considering three-dimensional magnetic field and slip boundary condition," *Proceedings of the Institution of Mechanical Engineers - Part E: Journal of Process Mechanical Engineering*, Article ID 095440892110464, 2021.

[14] M. Izady, S. Dinarvand, I. Pop, and A. J. Chamkha, "Flow of aqueous fe2o3–cuo hybrid nanofluid over a permeable stretching/shrinking wedge: a development on falkner–skan problem," *Chinese Journal of Physics*, vol. 74, pp. 406–420, 2021.

[15] T. Hayat, W. A. Khan, S. Z. Abbas, S. Nadeem, and S. Ahmad, "Impact of induced magnetic field on second-grade nanofluid flow past a convectively heated stretching sheet," *Applied Nanoscience*, vol. 10, no. 8, pp. 3001–3009, 2020.

[16] B. S. Goud, "Thermal radiation influences on mhd stagnation point stream over a stretching sheet with slip boundary conditions," *International Journal of Thermofluid Science and Technology*, vol. 7, no. 2, 2020.

[17] T. Srinivasulu and B. S. Goud, "Effect of inclined magnetic field on flow, heat and mass transfer of williamson nanofluid over a stretching sheet," *Case Studies in Thermal Engineering*, vol. 23, Article ID 100819, 2021.

[18] M. N. Khan and S. Nadeem, "A comparative study between linear and exponential stretching sheet with double stratification of a rotating Maxwell nanofluid flow," *Surfaces and Interfaces*, vol. 22, Article ID 100886, 2021.

[19] A. M. Spormann, "Unusual swimming behavior of a magnetotactic bacterium," *FEMS Microbiology Letters*, vol. 45, no. 1, pp. 37–45, 1987.

[20] A. Raees, H. Xu, and S.-J. Liao, "Unsteady mixed nano-bioconvection flow in a horizontal channel with its upper plate expanding or contracting," *International Journal of Heat and Mass Transfer*, vol. 86, pp. 174–182, 2015.

[21] S. Siddiqa, N. Begum, N. Begum, S. Saleem, M. Hossain, and R. S. Reddy Gorla, "Numerical solutions of nanofluid bioconvection due to gyrotactic microorganisms along a vertical wavy cone," *International Journal of Heat and Mass Transfer*, vol. 101, pp. 608–613, 2016.

[22] A. Abbasi, F. Mabood, W. Farooq, and M. Batool, "Bio-convective flow of viscoelastic nanofluid over a convective rotating stretching disk," *International Communications in Heat and Mass Transfer*, vol. 119, Article ID 104921, 2020.

[23] Y.-M. Chu, M. I. Khan, N. B. Khan et al., "Significance of activation energy, bio-convection and magnetohydrodynamic in flow of third grade fluid (non-Newtonian) towards stretched surface: a buongiorno model analysis," *International Communications in Heat and Mass Transfer*, vol. 118, Article ID 104893, 2020.

[24] M. B. Henda, H. Waqas, M. Hussain et al., "Applications of activation energy along with thermal and exponential space-based heat source in bioconvection assessment of magnetized third grade nanofluid over stretched cylinder/sheet," *Case Studies in Thermal Engineering*, vol. 26, Article ID 101043, 2021.

[25] S. A. Khan, H. Waqas, S. M. R. S. Naqvi, M. Alghamdi, and Q. Al-Mdallal, "Cattaneo-christov Double Diffusions Theories with Bio-Convection in Nanofluid Flow to Enhance the Efficiency of Nanoparticles Diffusion," *Case Studies In Thermal Engineering*, vol. 26, Article ID 101017, 2021.

[26] Y.-X. Li, M. H. Alshbool, Y.-P. Lv, I. Khan, M. Riaz Khan, and A. Issakhov, "Heat and mass transfer in mhd williamson nanofluid flow over an exponentially porous stretching surface," *Case Studies in Thermal Engineering*, vol. 26, Article ID 100975, 2021.

[27] A. Hamid, "Existence of dual solutions for wedge flow of magneto-williamson nanofluid: a revised model," *Alexandria Engineering Journal*, vol. 59, no. 3, pp. 1525–1537, 2020.

[28] G. Rasool, T. Zhang, A. J. Chamkha, A. Shafiq, I. Tlili, and G. Shahzadi, "Entropy generation and consequences of binary chemical reaction on mhd Darcy–forchheimer williamson nanofluid flow over non-linearly stretching surface," *Entropy*, vol. 22, no. 1, p. 18, 2019.

[29] A. Kumar, R. Tripathi, R. Singh, and V. Chaurasiya, "Simultaneous effects of nonlinear thermal radiation and joule heating on the flow of williamson nanofluid with entropy generation," *Physica A: Statistical Mechanics and Its Applications*, vol. 551, Article ID 123972, 2020.

[30] S. Shateyi and H. Muzara, "On the numerical analysis of unsteady mhd boundary layer flow of williamson fluid over a stretching sheet and heat and mass transfers," *Computation*, vol. 8, no. 2, p. 55, 2020.

[31] B. Ali, Y. Nie, S. A. Khan, M. T. Sadiq, and M. Tariq, "Finite element simulation of multiple slip effects on mhd unsteady Maxwell nanofluid flow over a permeable stretching sheet with radiation and thermo-diffusion in the presence of chemical reaction," *Processes*, vol. 7, no. 9, p. 628, 2019.

[32] T. N. Sindhu and A. Atangana, "Reliability analysis incorporating exponentiated inverse weibull distribution and inverse power law," *Quality and Reliability Engineering International*, vol. 37, no. 6, pp. 2399–2422, 2021.

[33] A. Rahman, T. N. Sindhu, S. A. Lone, and M. Kamal, "Statistical inference for burr type x distribution using geometric process in accelerated life testing design for time censored data," *Pakistan Journal of Statistics and Operation Research*, vol. 16, no. 3, pp. 577–586, 2020.

[34] A. Shafiq, S. Lone, T. N. Sindhu, Y. El Khatib, Q. M. Al-Mdallal, and T. Muhammad, "A new modified kies fréchet distribution: applications of mortality rate of covid-19," *Results in Physics*, vol. 28, Article ID 104638, 2021.

[35] T. N. Sindhu, A. Shafiq, and Q. M. Al-Mdallal, "Exponentiated transformation of gumbel type-ii distribution for modeling covid-19 data," *Alexandria Engineering Journal*, vol. 60, no. 1, pp. 671–689, 2021.

[36] A. Shafiq, A. B. Çolak, T. N. Sindhu, Q. M. Al-Mdallal, and T. Abdeljawad, "Estimation of unsteady hydromagnetic williamson fluid flow in a radiative surface through numerical and artificial neural network modeling," *Scientific Reports*, vol. 11, no. 1, Article ID 14521, 2021.

[37] A. Shafiq, A. B. Çolak, T. N. Sindhu, and T. Muhammad, "Optimization of Darcy-forchheimer squeezing flow in nonlinear stratified fluid under convective conditions with artificial neural network," *Heat Transfer Research*, vol. 53, no. 3, pp. 67–89, 2022.

[38] M. I. Asjad, M. Zahid, F. Jarad, and A. M. Alsharif, "Bio-convection flow of mhd viscous nanofluid in the presence of chemical reaction and activation energy," *Mathematical Problems in Engineering*, vol. 2022, Article ID 1707894, 9 pages, 2022.

[39] F. Wang, M. I. Asjad, S. U. Rehman et al., "Mhd williamson nanofluid flow over a slender elastic sheet of irregular thickness in the presence of bioconvection," *Nanomaterials*, vol. 11, no. 9, Article ID 2297, 2021.

[40] F. Mabood and S. Shateyi, "Multiple slip effects on mhd unsteady flow heat and mass transfer impinging on permeable stretching sheet with radiation," *Modelling and Simulation in Engineering*, vol. 2019, Article ID 3052790, 11 pages, 2019.